International Journal of Bifurcation and Chaos

CODIMENSION-3 BIFURCATION FOR CONTINUOUS SADDLE BIMODAL LINEAR DYNAMICAL SYSTEMS

JOSEP FERRER
Departament de Matemàtiques, Universitat Politècnica de Catalunya, Diagonal 647
08028 Barcelona, Spain
josep.ferrer@upc.edu

MARTA PEÑA
Departament de Matemàtiques, Universitat Politècnica de Catalunya, Diagonal 647
08028 Barcelona, Spain
marta.penya@upc.edu

ANTONI SUSIN
Departament de Matemàtiques, Universitat Politècnica de Catalunya, Diagonal 647
08028 Barcelona, Spain
toni.susin@upc.edu

Received (to be inserted by publisher)

We continue the study of the structural stability and the bifurcations of planar continuous bimodal linear dynamical systems (that is, systems consisting of two linear dynamics acting on each side of a straight line, assuming continuity along the separating line). Here, we complete the study when one of the subsystems is a saddle, leading to a 3D bifurcation diagram where a large catalogue of bifurcations appears: four surfaces of codimension-1 bifurcations; two sequences of surfaces of additional codimension-1 bifurcations; two lines of codimension-2 bifurcations; and one codimension-3 bifurcation.

Keywords: Piecewise linear system; structural stability; bifurcation diagram.

1. Introduction

Piecewise linear systems constitute a class of non-linear systems which have attracted the interest of researchers because of their interesting properties and the wide range of applications from which they arise. Even the planar continuous BLDS (planar continuous bimodal linear dynamical systems, that is, two planar linear subsystems acting in complementary halfplanes, assuming continuity in the separating straight line) have complex dynamic behaviors as well as applications (see, for example, [Artes *et al.*, 2013], [Camlibel *et al.*, 2003], [Di Bernardo *et al.*, 2008] and [Ferrer *et al.*, 2014]).

Our aim is a full characterization of the structurally stable planar continuous BLDS and a systematic study of the bifurcations between them, both in terms of the coefficients of the matrices which define the system. The structural stability of a system guarantees that its qualitative behavior is preserved under small perturbations of their parameters, whereas qualitative changes occur at the bifurcation points. We point out that both concepts (structural stability and bifurcation) depend on the equivalence relation which

precises the idea that two dynamical systems have the "same qualitative behavior". For example, for the equilibrium point of a single (non degenerate) planar linear system, those having positive trace and positive determinant form a unique (structurally stable) C^0-class (sources) whereas they are partitioned in four C^1-classes (spirals and nodes as structurally stable classes; improper nodes and starred nodes as bifurcations). Here we follow Sotomayor and Garcia [2003], where two planar continuous BLDS are equivalent if there is a homeomorphism of $\mathbf{R}^2$, preserving the separating line, which maps the orbits of a system into those of the other one and it is differentiable when restricted to finite periodic orbits. Then, general criteria are obtained by means of the Poincaré compactification which transforms the planar system into a system on the 2-sphere so that orbits at infinity can be considered. We maintain also the nomenclature in Sotomayor and Garcia [2003].

Till now, several partial studies exist concerning equilibrium points, periodic orbits or homoclinic orbits (see [Freire *et al.*, 1998], [Freire *et al.*, 2000], [Llibre *et al.*, 2013], [Xu *et al.*, 2013]). For example, in Xu et al. [2013] one specifies the conditions for the existence of saddle-loop orbits. In general, for planar continuous BLDS, in Freire et al. [1998] it is proved that there exists at most one saddle-loop orbit or limit cycle, which then must be attracting or repelling.

Our aim is a full integration of these and other behaviors in a complete bifurcation diagram, in particular analyzing their persistence under small perturbations. For this global study, the starting point is the reduced form of the matrices representing a continuous BLDS obtained in Ferrer et al. [2010].

Then, in Ferrer et al. [2014] we have specialized the general criteria for structural stability in Sotomayor and Garcia [2003] and we have pointed out that additional specific studies (concerning periodic orbits, saddle-loop (or homoclinic) orbits, saddle/tangency orbits and tangency/saddle orbits) are needed when one of the subsystems is a spiral. These previous results are collected in Section 2.

As a first goal, we focus our attention on the saddle/spiral case because it is the only one where all these elements can appear, so that more complex behaviors and applications are expected. In Ferrer et al. [2014] it becomes clear that in general the periodic orbits are structurally stable and that two bifurcations are possible for disappearing: an ordinary homoclinic bifurcation (when the trace τ of the spiral attains a certain value τ_H) and a special kind of Hopf bifurcation (when τ becomes 0). Indeed, in an ordinary Hopf bifurcation the periodic orbit collapses to the equilibrium point inside it, whereas in our case the spiral inside the periodic orbit does not collapse but changes from divergent to convergent, through a continuum of periodic orbits. In addition, in Ferrer et al. [2017] we prove that beyond both bifurcations there is not a zone of structural stability, but a sequence of saddle/tangency or tangency/saddle bifurcations, converging to the above homoclinic and Hopf bifurcations. Moreover, here we study the behavior of τ_H when the trace T of the saddle is near to 0. All these results concerning the saddle/spiral case are collected in Section 3.

Next, in Ferrer et al. [2016] we enlarge this study to the transformation of the considered spiral into a node, through an improper node. More precisely, we consider the trace of the spiral τ increasing till $\tau_0 \equiv 2\sqrt{\Delta}$ (where Δ is the determinant of the spiral, assumed constant): for $\mid \tau \mid = \tau_0$ the spiral becomes an improper node and for $\mid \tau \mid > \tau_0$ a structurally stable node. Moreover, one proves that $\mid \tau_H \mid \to \tau_0$ when the trace T of the saddle increases. These results are collected in Section 4.

Summarizing, the above results complete the study of the bifurcation diagram in the (τ, T)-plane, assuming constant both the determinants Δ and D of the right (spiral, node) and the left (saddle) subsystems, respectively. Here, in Section 5, we tackle the 3D bifurcation diagram when also Δ varies, dealing the right homogeneous subsystem to an improper node and a saddle, whereas D is assumed constant, so that we have a saddle as left subsystem. In future works also variation in D will be considered.

Other extensions are possible, such as considering nonlinear perturbations in some bifurcation. For example, it is well known that linear perturbations of a center give spirals, without limit cycles, whereas several limit cycles can appear if nonlinear perturbations are considered. In our case, Fig. 6 shows that linear perturbations of a center (in a half-plane) give just one limit cycle (or a spiral). We expect that several limit cycles, placed inside the above one, can be obtained by means of nonlinear perturbations.

More specifically, we describe the codimension-1 bifurcation (saddle/degenerate node) when $\Delta = 0$ (and $\tau \neq 0$), the codimension-2 bifurcation (saddle/improper degenerate node) when $\Delta = \tau = 0$ (and $T \neq 0$), and the codimension-3 bifurcation when $\Delta = \tau = T = 0$. We remark that in any neighborhood of the last one, all other bifurcations appear. They are listed in Section 6 and collected in the 3D bifurcation

diagram (τ, T, Δ) in Fig. 11.

Throughout the paper, $\mathbf{R}$ will denote the set of real numbers, $M_{n\times m}(\mathbf{R})$ the set of matrices having n rows and m columns and entries in $\mathbf{R}$ (in the case where $n = m$, we will simply write $M_n(\mathbf{R})$) and $Gl_n(\mathbf{R})$ the group of non-singular matrices in $M_n(\mathbf{R})$. Finally, we will denote by $e_1, \ldots, e_n$ the natural basis of the Euclidean space $\mathbf{R}^n$.

2. Structural stability of planar bimodal linear systems

Let us consider a bimodal linear dynamical system (BLDS) given by two subsystems each one acting in a halfspace:

$$\dot{x}(t) = A_1 x(t) + B_1 \qquad \text{if } Cx(t) \leq 0,$$

$$\dot{x}(t) = A_2 x(t) + B_2 \qquad \text{if } Cx(t) \geq 0,$$

where $A_1, A_2 \in M_n(\mathbf{R})$; $B_1, B_2 \in M_{n\times 1}(\mathbf{R})$; $C \in M_{1\times n}(\mathbf{R})$. We assume that the dynamics is continuous along the separating hyperplane $H = \{x \in \mathbf{R}^n : Cx = 0\}$; namely, that both subsystems coincide for $Cx(t) = 0$.
By means of a linear change in the state variable $x(t)$, we can consider $C = (1\ 0 \ldots 0) \in M_{1\times n}(\mathbf{R})$. Hence $H = \{x \in \mathbf{R}^n : x_1 = 0\}$ and continuity along H is equivalent to:

$$B_2 = B_1, \qquad A_2 e_i = A_1 e_i, \quad 2 \leq i \leq n.$$

We will write from now on $B = B_1 = B_2$.

Definition 2.1. Under the above conditions, we say that the triple of matrices (A_1, A_2, B) defines a *continuous bimodal linear dynamical system (CBLDS).*

Thus, we consider in the set of CBLDS the natural topology as a $(n^2 + n^2 + n)$-dimensional euclidean space. Our goal is to characterize the planar CBLDS which are structurally stable in the sense of [Sotomayor & Garcia, 2003] in terms of the coefficients A_1, A_2 and B, and to analyze the bifurcations appearing in the boundary values between them. So, from now on we specialize to $n = 2$.

The placement of the equilibrium points will play a significative role in the dynamics of a CBLDS. So, we define:

Definition 2.2. Let us assume that a subsystem of a CBLDS has a unique equilibrium point, not lying in the separating line. We say that this equilibrium point is *real* if it is located in the halfplane corresponding to the considered subsystem. Otherwise, we say that the equilibrium point is *virtual.*

A natural tool in the study of CBLDS is simplifying the matrices A_1, A_2, B by means of changes in the variables $x(t)$ which preserve the qualitative behavior of the system (in particular, the condition of structural stability). So, we consider linear changes in the state variables space preserving the hyperplanes $x_1(t) = k$, which will be called *admissible basis changes.* See [Ferrer *et al.*, 2010] for the resulting reduced forms. Also, translations parallel to the separating line H are allowed. Then, by specializing to CBLDS the general necessary and sufficient conditions in Sotomayor and Garcia [2003], in Ferrer et al. [2014] one proves the following results.

Theorem 1. *[Ferrer et al., 2014] Let us consider planar CBLDS.*

(1) If such a CBLDS is structurally stable, then the triples of matrices representing it can be reduced (by means of an admissible basis change and a translation parallel to the separating line) to the form:

$$A_1 = \begin{pmatrix} T & 1 \\ -D & 0 \end{pmatrix}, A_2 = \begin{pmatrix} \tau & 1 \\ -\Delta & 0 \end{pmatrix}, B = \begin{pmatrix} 0 \\ b \end{pmatrix}, b \neq 0$$

In particular, the only tangency point (i.e., where an orbit and the separating line are tangent) is $(0, 0)$.

(2) If one of the subsystems is a center, a degenerate node, an improper node or a starred node, then the CBLDS is not structurally stable.

(3) For the remainder CBLDS, if none subsystem is a real spiral then the CBLDS is structurally stable. Explicitly (for $b > 0$; when $b < 0$, we obtain the symmetric ones) when:
the left subsystem is a real saddle, a virtual node or a virtual spiral
the right subsystem is a virtual saddle or a real node
(4) Additional conditions must be verified if one of the subsystems is a real spiral (in the right halfplane if $b > 0$):
(4.1) A CBLDS real saddle/real spiral is structurally stable if and only if:
(a) the finite periodic orbits are hyperbolic
(b) there are not saddle-loop orbits
(c) there are not finite orbits connecting a saddle and a tangency point
(4.2) A CBLDS virtual node/real spiral is structurally stable if and only if condition (a) holds
(4.3) A CBLDS virtual spiral/real spiral is structurally stable if and only if condition (a) holds and also:
(a') the infinite periodic orbit at infinity is hyperbolic

Remark 2.1. In (1) of the above Theorem one can take $b = 1$ (by means of a change of scale and a symmetry, if necessary), but we will consider general $b \neq 0$ because of the homogeneity in the obtained formulas.

Remark 2.2. Because of (1) of the above Theorem, we will not consider starred nodes nor null subsystems.

3. The saddle/spiral case

Concerning the case (4.1) in Theorem 1, conditions (a) and (b) have been studied in [Ferrer *et al.*, 2014] and condition (c) in [Ferrer *et al.*, 2017]. First, we summarize the results in [Ferrer *et al.*, 2014] concerning this case (4.1). Moreover, we precise the uniqueness of the finite periodic orbit in (3) (see [Freire *et al.*, 1998]).

Theorem 2. *[Ferrer et al., 2014] Let us assume the case (4.1) above, that is:*

$$b > 0, D < 0, \Delta > 0, \tau^2 < 4\Delta$$

in (1) of Theorem 1, and let

$$\lambda_2 < 0 < \lambda_1 \quad \textit{be the eigenvalues of } A_1, \textit{and}$$

$$\alpha \pm i\beta, \beta > 0, \quad \textit{be the eigenvalues of } A_2.$$

Then, for $\tau > 0$:

(1) If $T \geq 0$, then there are not homoclinic orbits nor finite periodic orbits.
(2) If $T < 0$, a homoclinic (i.e., saddle-loop) orbit appears only for a value τ_H of τ satisfying $0 < \tau_H < \frac{T\Delta}{D}$.
(3) If $T < 0$, a unique finite periodic orbit exists for $0 < \tau < \tau_H$, being attractive hyperbolic (and transverse to the separating axis). No saddle/tangency orbits exist.

Corollary 3.1. *[Ferrer et al., 2014] Under the conditions of Theorem 2, the systems with $T < 0$ and $0 < \tau < \tau_H$ are structurally stable.*

Example 3.1. For $D = -1$, $\Delta = 5$, $T = -1$ and $b = 1$ one obtains $\tau_H = 0.742$ (see Fig. 10). Finite periodic orbits appear in Fig. 6 and Fig. 7, for $\tau = 0.172$ and $\tau = 0.1$, respectively.

The following theorem specifies the value of τ_H.

Theorem 3. *[Xu et al., 2013] Under the conditions of Theorem 2, τ_H is the value of τ satisfying*

$$\frac{1}{2}\ln\left(\frac{\lambda_2^2}{\lambda_1^2}\frac{\lambda_1^2 - \tau\lambda_1 + \Delta}{\lambda_2^2 - \tau\lambda_2 + \Delta}\right) - \frac{\alpha}{\beta}\left(2\pi - \arctan\frac{\lambda_2\alpha - \Delta}{\lambda_2\beta} - \arctan\frac{\Delta - \lambda_1\alpha}{\lambda_1\beta}\right) = 0. \qquad Eq.(1)$$

Remark 3.1. For $\tau < 0$ one has symmetric results:

(1') If $T \leq 0$, there are not homoclinic orbits nor finite periodic orbits.
(2') If $T > 0$, the only homoclinic orbit appears for a unique value τ_H of τ satisfying $\frac{T\Delta}{D} < \tau_H < 0$.
(3') If $T > 0$, a unique finite periodic orbit exists for each $\tau_H < \tau < 0$, being hyperbolic (and transverse to the separating axis). Hence, the system is structurally stable.

We can precise the behavior of τ_H near $T = 0$.

Proposition 1. *Under the above conditions, we fix D, Δ and b. Then:*

(1) $\tau_H \to 0$, when $T \to 0$. Hence, at $T = \tau = 0$ one has a codimension-2 bifurcation, which is a limit point of the codimension-1 bifurcations $\tau = 0$ and $\tau = \tau_H$.
(2) $\tau_H(T)$ cuts transversally the axis $\tau = 0$ at $T = 0$. Indeed, its derivative at the origin is:

$$\frac{\partial \tau_H}{\partial T}(0) = \frac{-\Delta\mu}{\mu - (D-\Delta)(\pi - \arctan \mu)} < 0 \qquad Eq.(2)$$

where $\mu = \sqrt{\frac{\Delta}{-D}}$.

Proof. (1) is obvious from $0 < \tau_H < \frac{T\Delta}{D}$.
For (2), bearing in mind Eq. (1) in Theorem 3, we consider the equations
$\tau = 2\alpha$
$\alpha^2 + \beta^2 = \Delta$
$\lambda_1\lambda_2 = D$
$\lambda_1 + \lambda_2 = T$
$\frac{1}{2}\ln(\frac{\lambda_2^2}{\lambda_1^2}\frac{\lambda_1^2 - \tau\lambda_1 + \Delta}{\lambda_2^2 - \tau\lambda_2 + \Delta}) - \frac{\alpha}{\beta}(2\pi - \arctan\frac{\lambda_2\alpha - \Delta}{\lambda_2\beta} - \arctan\frac{\Delta - \lambda_1\alpha}{\lambda_1\beta}) = 0$

or, equivalently, we consider $f(\lambda_1, \beta, \tau, T) = (f_1, f_2, f_3)$, being
$f_1 = \tau^2/4 + \beta^2 - \Delta$
$f_2 = \lambda_1 + D/\lambda_1 - T$
$f_3 = \frac{1}{2}\ln(\frac{D^2}{\lambda_1^2}\frac{\lambda_1^2 - \tau\lambda_1 + \Delta}{D^2 - 2D\lambda_1 + \Delta\lambda_1^2}) - \frac{\tau}{2\beta}(2\pi - \arctan\frac{\frac{D\tau}{2} - \Delta\lambda_1}{D\beta} - \arctan\frac{\Delta - \frac{\lambda_1\tau}{2}}{\lambda_1\beta})$

Then, the equation $f(\lambda_1, \beta, \tau, T) = (0, 0, 0)$ defines (λ_1, β, τ) as implicit functions of T.
Since

$$\frac{\partial(\lambda_1, \beta, \tau)}{\partial T} = -(\frac{\partial f}{\partial(\lambda_1, \beta, \tau)})^{-1}\frac{\partial f}{\partial T}$$

one has that if $(\lambda_1, \beta, \tau, T) = (\sqrt{-D}, \sqrt{\Delta}, 0, 0)$ then

$$\frac{\partial \tau}{\partial T} = \frac{\frac{\partial f_3}{\partial \lambda_1}}{-2\frac{\partial f_3}{\partial \tau}}$$

$$\frac{\partial f_3}{\partial \lambda_1} = \frac{2\Delta}{\sqrt{-D}(D - \Delta)}$$

$$\frac{\partial f_3}{\partial \tau} = \frac{-\sqrt{-D}}{D(D-\Delta)} - \frac{1}{\sqrt{\Delta}}(\pi - \arctan\sqrt{\frac{\Delta}{-D}})$$

and taking $\mu = \sqrt{\frac{\Delta}{-D}}$ we get the formula Eq. (2) for $\frac{\partial \tau_H}{\partial T}(0)$. ■

Example 3.2. If we consider, as in the above example, $D = -1$ and $\Delta = 5$, then $\mu = \sqrt{5}$, and in this case Eq. (2) gives $\frac{\partial \tau_H}{\partial T}(0) = \frac{-5\sqrt{5}}{\sqrt{5} + 6(\pi - \arctan\sqrt{5})} = -0.7882$.

Next, we summarize the results in [Ferrer *et al.*, 2017] concerning condition (c).

First, we tackle the values $\tau > \tau_H$. We will see that there is a decreasing sequence $\tau_1, \tau_2, ... \to \tau_H$ of values of τ where tangency/saddle singularities appear. For the remainder values, the CBLDS is structurally stable.

Theorem 4. *[Ferrer et al., 2017] Under the conditions of Theorem 2, let us consider $T < 0$ and $\tau > \tau_H (> 0)$:*

1. *There exists a maximal value τ_1 of τ (see Fig. 8), for which a tangency/saddle orbit appears. Moreover, $\tau_1 < \frac{\Delta}{\lambda_1}$.*

2. *There exists a decreasing sequence $(\tau_1, \tau_2, ..., \tau_k, ...) \to \tau_H$, $k \geq 1$, for which tangency/saddle orbits appear.*
   For the value $\tau = \tau_k$ the orbit through the tangency point $(0, 0)$ has its $(2k-1)$th intersection with the separating line just at $(0, -b/\lambda_1)$, going later to the saddle equilibrium point. See Figure 8.
3. *For the remainder values of $\tau > \tau_H$, the CBLDS is structurally stable. For $\tau_{k+1} < \tau < \tau_k$ (respectively $\tau > \tau_1$), the tangent orbit goes to infinity after crossing the separating line $2k+1$ (respectively, 1) times. See Figure 7.*

In an analogous way, for $\tau < 0$ there is an increasing sequence $\tau_{-1}, \tau_{-2}, ... \to 0$ of values of τ where saddle/tangency singularities appear.

Theorem 5. *[Ferrer et al., 2017] Under the conditions of Theorem 2, let us consider $T < 0$ and $\tau < 0$:*

1. *There exists a minimal value τ_{-1} of τ (see Fig. 9), for which a saddle/tangency orbit appears. Moreover, $\tau_{-1} > \frac{\Delta}{\lambda_2}$.*

2. *There exists an increasing sequence $(\tau_{-1}, \tau_{-2}, ..., \tau_{-k}, ...) \to 0$, $k \geq 1$, for which saddle/tangency orbits appear.*
   For the value $\tau = \tau_{-k}$ the orbit through $(0, -b/\lambda_2)$ has its $(2k-1)$th intersection with the separating line just at the origin.
3. *For the remainder values of $\tau < 0$, the CBLDS is structurally stable.*

Clearly $\lambda_2 \to -\infty$ when $T \to -\infty$. Hence:

Corollary 3.2. *Under the above conditions:*

$\tau_{-1} \to 0$, when $T \to -\infty$.

Remark 3.2. For $T > 0$ one has symmetric results:

(1') For $\tau < \tau_H$:
- There exists a minimal value of τ, τ_{-1}, for which a tangency/saddle orbit appears, satisfying $\tau_{-1} > \frac{\Delta}{\lambda_2}$.
- There exists an increasing sequence $(\tau_{-1}, \tau_{-2}, ..., \tau_{-k}, ...) \to \tau_H$, $k \geq 1$, for which tangency/saddle orbits appear.
- For the remainder values of $\tau < \tau_H$, the CBLDS is structurally stable.

(2') For $\tau > 0$:
- There exists a maximal value of τ, τ_1, for which a saddle/tangency orbit appears, satisfying $\tau_1 < \frac{\Delta}{\lambda_1}$.
- There exists a decreasing sequence $(\tau_1, \tau_2, ..., \tau_k, ...) \to 0$, $k \geq 1$, for which saddle/tangency orbits appear.
- For the remainder values of $\tau > 0$, the CBLDS is structurally stable.
- $\tau_1 \to 0$, when $T \to +\infty$.

4. The bifurcation at an improper node

The spiral in the above section becomes a node when $|\tau| \geq \tau_0 \equiv 2\sqrt{\Delta}$, with a bifurcation appearing for $|\tau| = \tau_0$, where the right subsystem is an improper node (see Remark 6.)

Let us consider a BLDS (A_1, A_2, B) as in (1) of Theorem 1, with

$$D < 0, \Delta > 0, b > 0,$$

that is, the left subsystem is a real saddle and the right one is a real node or spiral. From Theorem 4, we have

Proposition 2. *[Ferrer et al., 2016] Under the above conditions, let* $\tau_0 = 2\sqrt{\Delta}$. *Then:*

(1) For $\mid \tau \mid > \tau_0$ *one has a structurally stable system saddle/node.*
(2) For $\mid \tau \mid = \tau_0$ *one has a bifurcation saddle/improper node.*
(3) For $\mid \tau_H \mid < \mid \tau \mid < \tau_0$ *one has a system saddle/spiral, which is structurally stable if no tangency/saddle nor saddle/tangency orbits appear.*

Remark 4.1. For $\mid \tau_H \mid < \mid \tau \mid < \tau_0$ in (3) above, see Theorems 4 and 5. Notice also the following result.

Example 4.1.

We include figures of the transition $\mid \tau_H \mid < \mid \tau \mid < \tau_0$, $\mid \tau \mid = \tau_0$, $\mid \tau \mid > \tau_0$ for $T = 1, D = -1, \Delta = 5$ and $b = 1$, so that $\tau_0 = 2\sqrt{5} = 4.4721$, $\tau_H = -0.742$.

More precisely, Figure 1 (a) corresponds to $\tau = -1.9721$ (saddle/spiral). Notice that the tangent orbit (as well as the ones over the saddle/spiral orbit) intersects the separating line in just an additional point. The remainder orbits intersect twice in the main quadrant of the saddle and a third time over it.

Figure 1 (b) corresponds to $\tau = -4.4721$ (saddle/improper node). Now the tangent orbit does not intersect the separating line because it cannot cross the new invariant line arising from the equilibrium point of the improper node, placed at $(0.2, 0.8944)$.

In Figure 1 (c), corresponding to $\tau = -7.9721$ (saddle/node), this invariant line splits into two of them, giving an ordinary node, placed at $(0.2, 1.5944)$.

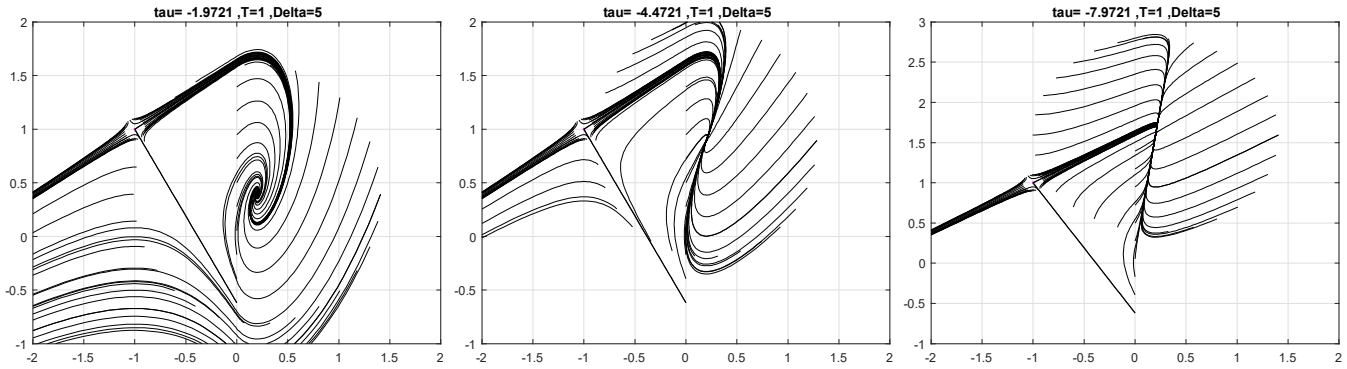

Fig. 1. From left to right, figures corresponding to Example 4.1: $\tau = -1.9721 > -\tau_0$ (a), $\tau = -\tau_0 = -4.4721$ (b), $\tau = -7.9721 < -\tau_0$ (c)

Therefore, the (τ, T) bifurcation diagram in Ferrer et al. [2017](see Figure 2) can be enlarged to $-\tau_0 \leq \tau \leq \tau_0$, bearing in mind the following proposition.

Proposition 3. *[Ferrer et al., 2016] In the above conditions:*

(1) $\tau_H \to -\tau_0$, *when* $T \to +\infty$.
(2) $\tau_H \to \tau_0$, *when* $T \to -\infty$.

5. The bifurcation at a degenerate node

Till now one has considered constant the determinant Δ of the subsystem in the right halfspace (a spiral or a node). Now we will vary Δ starting from a saddle/node BLDS, that is, $0 < \Delta < \tau^2/4$.

If Δ increases, at $\Delta = \frac{\tau^2}{4}$ one finds again an improper node bifurcation as in Section 4, leading to a structurally stable saddle/spiral.

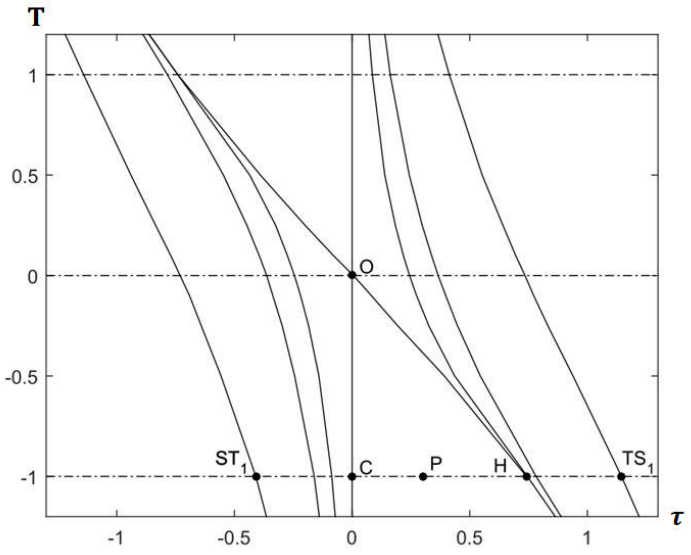

Fig. 2. Bifurcation diagram in the (τ, T)-plane

Now, if Δ decreases, the right homogeneous subsystem becomes a degenerate node for $\Delta = 0$ and the equilibrium point goes to infinity (it can be seen as a "node at infinity": see Figure 3 (b)). Next, for $\Delta < 0$, the right subsystem becomes a virtual saddle (its equilibrium point will lie in the left halfspace), being structurally stable the resulting real saddle/virtual saddle CBLDS (see Figure 3 (c)).

Proposition 4. *Let us assume*

$$b > 0, D < 0, \Delta < \frac{\tau^2}{4}, \tau \neq 0.$$

Then, for any T:

(1) For $\Delta = 0$ one has a bifurcation saddle/degenerate node (or "node at infinity").
(2) For $\Delta > 0$ (and $\Delta < \frac{\tau^2}{4}$) one has a structurally stable saddle/node.
(3) For $\Delta < 0$ one has a structurally stable real saddle/virtual saddle.

Example 5.1.

We include figures of the transition $\Delta < 0, \Delta = 0, \Delta > 0$ for $T = 1, D = -1, \tau = -4.4721, b = 1$.

More precisely, Figure 3 (a) corresponds to $\Delta = 3 < \frac{\tau^2}{4} = 5$ (saddle/node), as in the above example. It is equivalent to Figure 1 (c), but now the node is placed at $(0.3333, 1.4907)$.

Figure 3 (b) corresponds to nearly $\Delta = 0$ (saddle/degenerate node) without changes in the remaining parameters. Then the equilibrium point in the right subsystem goes to infinity, so that the orbits there become nearly parallel.

Figure 3 (c) corresponds to $\Delta = -20$ (real saddle/virtual saddle), again without changes in the remaining parameters: the right subsystem is a saddle, having its equilibrium point at $(-0.2, 0.2236)$ in the left halfplane.

Notice that, when $\Delta > 0$ decreases, also $\tau_0 = 2\sqrt{\Delta}$ decreases, so that the (τ, T) bifurcation diagram in Figure 2 becomes more and more narrow, till the axis $\tau = 0$ for $\Delta = 0$ (and empty for $\Delta < 0$). Therefore, the line $\Delta = \tau = 0$ is a quite complex codimension-2 bifurcation: it is the limit of all bifurcation sets (H,C,TS_k, ST_k) in Figure 2; also it is the limit of the degenerate nodes $\Delta = 0$, $\tau \neq 0$, in this section; indeed the right homogeneous subsystem is a degenerate improper node (at infinity, as above) of the form

$$A_2 = \begin{pmatrix} 0 & 1 \\ 0 & 0 \end{pmatrix}, B = \begin{pmatrix} 0 \\ b \end{pmatrix}, b \neq 0$$

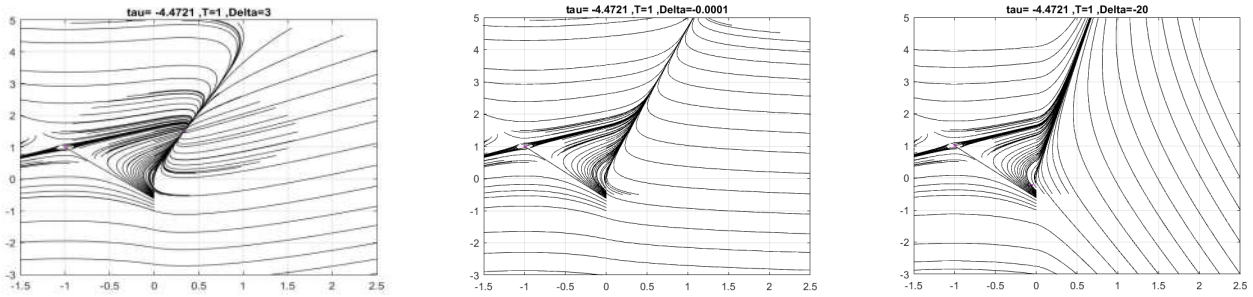

Fig. 3. From left to right, figures corresponding to Example 5.1: $\Delta = 3$ (a), $\Delta = -0.0001$ (b), $\Delta = -20$ (c)

Proposition 5. *Let us assume*

$$b > 0, D < 0, T \neq 0.$$

Then, for $\Delta = \tau = 0$ one has a codimension-2 bifurcation saddle/degenerate improper node. It is a limit point of all the above codimension-1 bifurcations in Section 3 ($\tau = 0, \tau = \tau_H, \tau = \tau_k, \tau = \tau_{-k}, k = 1, 2, ...$), in Section 4 ($4\Delta = \tau^2$) and in Proposition 4 ($\Delta = 0$).

Example 5.2. Figure 4 corresponds to $D = -1, T = 1, b = 1$ and nearly $\Delta = 0$ and $\tau = 0$.

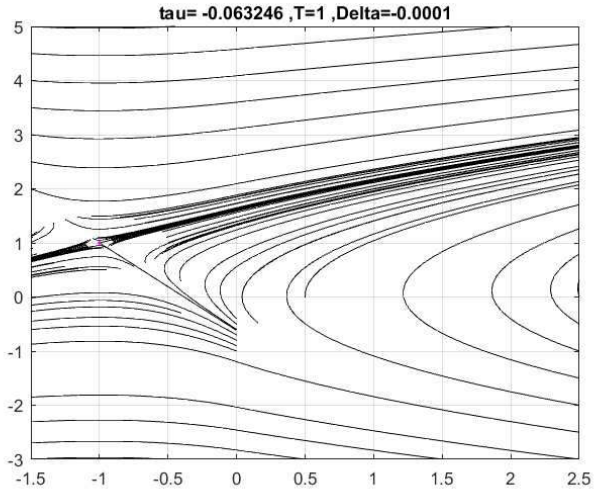

Fig. 4. Corresponding to the degenerate improper node bifurcation, $\Delta = 0.001$, $\tau = -0.0632$ ($D = -1$, $T = 1$, $b = 1$)

If in addition $T = 0$, then the saddle in the left halfspace becomes symmetric, so that also the bifurcation set $\tau = T = 0$ in Proposition 1 converges to it.

Proposition 6. *Let us assume*

$$b > 0, D < 0.$$

Then, for $T = \Delta = \tau = 0$ one has a codimension-3 bifurcation symmetric saddle/degenerate improper node, which is a limit point of all the codimension-1 bifurcations above, as well as the codimension-2 bifurcations $\Delta = \tau = 0$ in Proposition 5 and the codimension-2 bifurcation $T = \tau = 0$ in Proposition 1.

Example 5.3. Figure 5 corresponds to $T = \Delta = \tau = 0, D = -1, b = 1$.

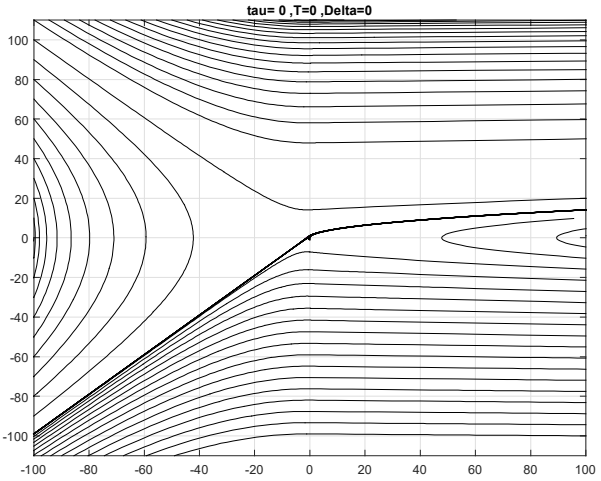

Fig. 5. Corresponding to the (OO)-bifurcation, $\Delta = \tau = T = 0$ ($D = -1, b = 1$)

6. The 3D bifurcation diagram when the left subsystem is a saddle

Putting together the above results, one obtains the 3D bifurcation diagram in Figure 11, where the horizontal axes are the trace τ and the determinant Δ of the right subsystem, whereas the vertical axis is the trace T of the saddle in the left halfplane (its determinant D is assumed constant, $D = -1$).

So, the right subsystem is a degenerate node in the vertical plane $\Delta = 0$ and a saddle in the back halfplane $\Delta < 0$. In the front halfspace $\Delta > 0$, the parabolic cylinder $\tau^2 = 4\Delta$ corresponds to improper nodes, the points outside it ($0 < \Delta < (\tau^2/4)$) correspond to nodes and the ones inside the parabolic cylinder ($\Delta > (\tau^2/4)$) correspond to spirals if $\tau \neq 0$ and centers if $\tau = 0$.

6.1. *The saddle/spiral bifurcations*

In the planes Δ =constant ($\Delta = 5$ in the figure), inside the parabolic cylinder (that is, $\mid \tau \mid < \tau_0 \equiv 2\sqrt{\Delta}$) one has the (T, τ)-diagram in [Ferrer *et al.*, 2017]. Summarizing:

6.1.1. *The hyperbolic periodic orbits*

For $0 <\mid \tau \mid <\mid \tau_H \mid$, such as P in the figure, a unique hyperbolic periodic orbit appears. For example, the periodic orbit for $\tau = 0.1$ in Figure 7 and $\tau = 0.172$ in Figure 6, both for $T = -1, D = -1, \Delta = 5, b = 1$ (being $\tau_H = 0.742$).

6.1.2. *The (C)-bifurcations*

For $\tau = 0$, one has a kind of degenerate Hopf bifurcation: the periodic orbit above becomes tangent to the separating line, and the ones inside it form a continuum of (non-hyperbolic) periodic orbits. See the transition in Figure 6.

6.1.3. *The (H)-bifurcations*

For $\tau = \tau_H$, one has a bifurcation similar to the classical homoclinic ones: the periodic orbit for $\tau < \tau_H$ (see (5.1.1)) becomes a saddle-loop orbit. See the transition in Figure 7.

6.1.4. *The tangency/saddle bifurcations (TS_k)*

There is a decreasing sequence $\tau_1, \tau_2, \tau_3, ...$ (converging to τ_H if $T \leq 0$ or to 0 if $T \geq 0$) where the tangent orbit (at the origin) goes to the saddle equilibrium point, after crossing the separating line 1,3,5,... times respectively. See Figure 8 (where $\tau_H = 0.742$.)

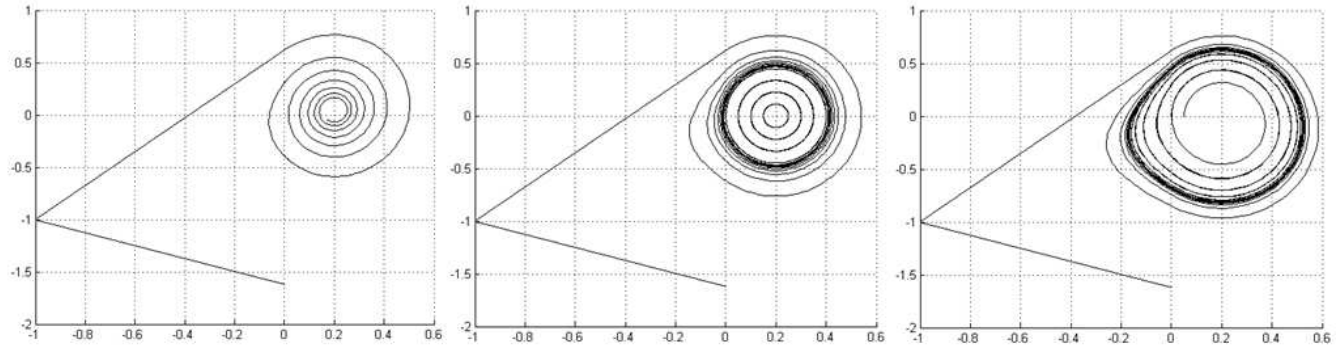

Fig. 6. From left to right, the (C)-transition corresponding to values: $\tau = -0.2$, $\tau = 0$, $\tau = 0.172$ ($D = -1$, $\Delta = 5$, $T = -1$, $b = 1$)

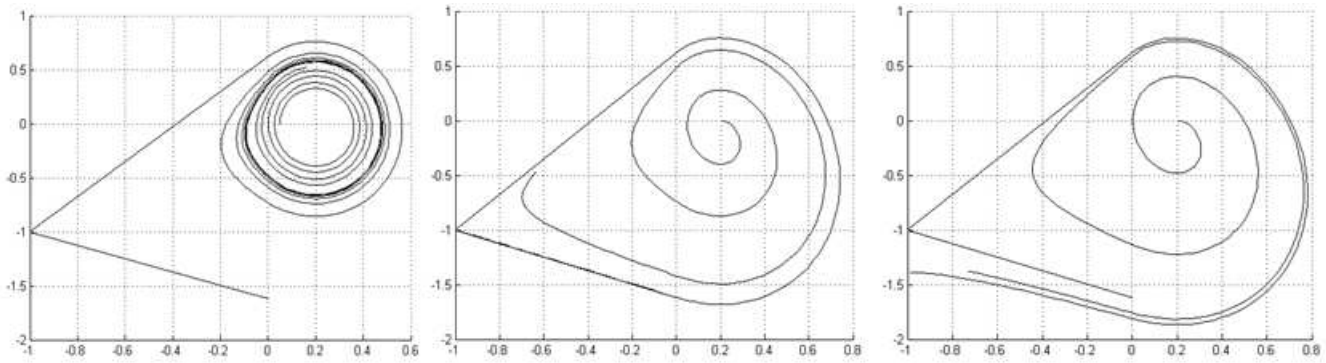

Fig. 7. From left to right, the (H)-transition corresponding to values: $\tau = 0.1$, $\tau = \tau_H = 0.742$, $\tau = 0.85$ ($D = -1$, $\Delta = 5$, $T = -1$, $b = 1$)

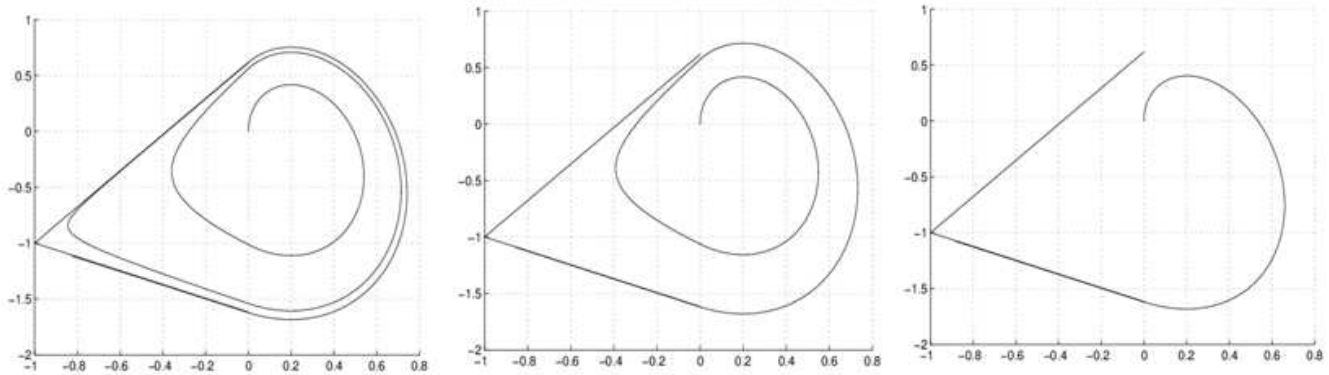

Fig. 8. From left to right, the tangency/saddle orbits corresponding to values: $\tau_3 = 0.745, \tau_2 = 0.782, \tau_1 = 1.145$ ($D = -1$, $\Delta = 5$, $T = -1$, $b = 1$)

For $\tau_{k+1} < \tau < \tau_k$ (respectively, $\tau_1 < \tau < \tau_0$), the tangent orbit goes to infinity, after crossing the separating line $2k + 1$ times (respectively, 1 time.) See in Figure 7, $\tau_2 < \tau = 0.85 < \tau_1$.

6.1.5. *The saddle/tangency bifurcations (ST_k)*

Analogously, there is an increasing sequence $\tau_{-1}, \tau_{-2}, ...$ (converging to τ_H if $T \geq 0$ or to 0 if $T \leq 0$) where the tangent orbit comes from the saddle equilibrium point, crossing the separating line 1,3,... times respectively. See in Figure 9, $\tau_{-1} = -0.409$.

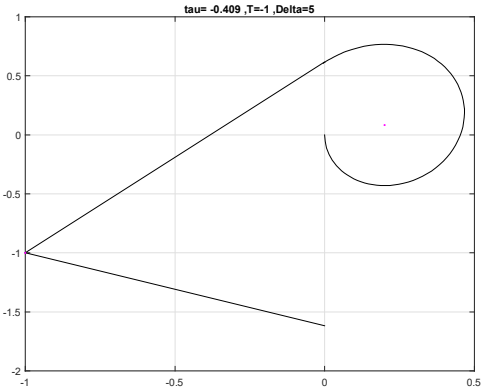

Fig. 9. Corresponding to a saddle/tangency orbit, $\tau_{-1} = -0.409$ ($D = -1$, $\Delta = 5$, $T = -1$, $b = 1$)

6.1.6. *The (O)-bifurcation*

For $\tau = T = 0$, a codimension-2 bifurcation appears: a saddle-loop, being (non hyperbolic) periodic all the orbits inside it. See Figure 10.

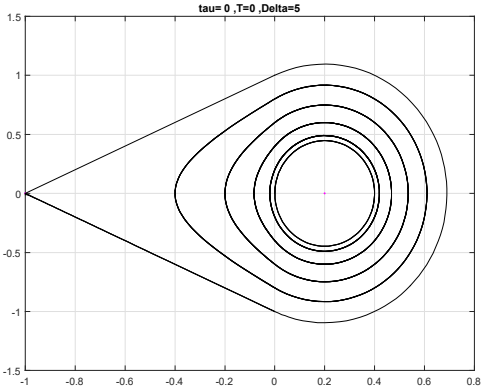

Fig. 10. Corresponding to the (O)-bifurcation, $\tau = T = 0$ ($D = -1$, $\Delta = 5$, $b = 1$)

6.2. *The saddle/node bifurcations*

As we have seen, new bifurcations appear when the points on the parabolic cylinder or outside it are considered.

6.2.1. *The improper node bifurcation (IN)*

In Section 4 we have enlarged the study in Section 6.1 to $\mid \tau \mid \geq \tau_0 \equiv 2\sqrt{\Delta}$, that is to say, to the whole (T, τ)-plane Δ =constant: the spiral in the right halfplane for $\mid \tau \mid < \tau_0$ becomes a node for $\mid \tau \mid > \tau_0$, a bifurcation appearing at $\mid \tau \mid = \tau_0$, where the right subsystem is an improper node (Remark 5). See Figure 1 (b) (where $D = -1$, $\Delta = 5$, $T = -1$, $b = 1$).

6.2.2. *The degenerate node bifurcation (DN)*

Till now, we have considered $\Delta > 0$, constant. Now we consider decreasing values of Δ. Bearing in mind 6.2.1, we may assume the starting point outside the parabolic cylinder $\tau^2 = 4\Delta$, if $\tau \neq 0$. Clearly, the node in the right halfplane will become a saddle for $\Delta < 0$, towards a degenerate node (a "node at infinity") for $\Delta = 0$. See Figure 3 (b) (where $\tau = -4.4721$, $T = 1$, $b = 1$).

6.2.3. *The degenerate improper node bifurcation (DIN)*

A codimension-2 bifurcation appears when $\Delta = \tau = 0$ ($T \neq 0$) where the parabolic cylinder $\tau^2 = 4\Delta$ and the plane $\Delta = 0$ are tangent: the right homogeneous subsystem is a degenerate improper node (Remark 5). See Figure 4 (where $T = 1$, $b = 1$).

6.3. *The codimension-3 (OO)-bifurcation*

Finally, see Figure 5 for $\Delta = \tau = T = 0$: the particular case of (6.2.3) when the saddle in the left halfplane is symmetric. Notice that in any neighborhood of it, all the other cases occur, both the structurally stable, as well as all the bifurcations above.

7. Conclusion

We complete the study of the structural stability and the bifurcations of planar bimodal linear dynamical systems when the left subsystem is a saddle. It gives a 3D bifurcation diagram containing a large catalogue of codimension 1, 2 and 3 bifurcations. The axes are the traces of both subsystems and the determinant of the right one, assuming constant the determinant of the saddle in the left halfplane.

The study starts from the definition of structural stability and the basic conditions for it in Sotomayor and Garcia [2003]. By means of the reduced forms in Ferrer et al. [2010], one studies the saddle/spiral case in Ferrer et al. [2014] (periodic orbits) and Ferrer et al. [2017] (saddle/tangency and tangency/saddle orbits.) This study is enlarged in Ferrer et al. [2016] when the right subsystem is a node. Here we complete it (a saddle in the right halfplane, new codimension-2 bifurcations, transversality of some bifurcation surfaces,...) and we put together all the results in the referred 3D bifurcation diagram.

Acknowledgements: The research is supported by MTM2015-68805-REDT of ALAMA net (first and second author) and TIN2014-52211-C2-1-R partially supported by the Spanish Ministerio E&C and FEDER founding (third author).

We are very grateful to the Editors and Reviewers for their valuable comments and suggestions.

References

Artes, J., Llibre, J., Medrado, J.C. & Teixeira, M.A. [2013] "Piecewise linear differential systems with two real saddles," *Math. Comput. Simul.* **95**, 13–22.

Camlibel, K., Heemels, M. & Schumacher, H. [2003] "Stability and controllability of planar bimodal linear complementarity systems," *Proc. IEEE Conf. Decis. Control*, pp. 1651–1656.

Di Bernardo, M., Pagano, D. J. & Ponce, E. [2008] "Nonhyperbolic boundary equilibrium bifurcations in planar Filippov systems: a case study approach," *Int. J. Bifurcation and Chaos* **18**, 1377–1392.

Ferrer, J., Magret, M. & Peña, M. [2010] "Bimodal piecewise linear systems. Reduced forms," *Int. J. Bifurcation and Chaos* **20**, 2795–2808.

Ferrer, J., Magret, M. & Peña, M. [2014] "Differentiable Families of Planar Bimodal Linear Control Systems," *Math. Probl. Eng.*, 292813, 1–9.

Ferrer, J., Peña, M. & Susin, A. [2014] "Structural stability of planar bimodal linear systems," *Math. Probl. Eng.*, 892948, 1–8.

Ferrer, J., Peña, M. & Susin, A. [2016] "Bifurcation diagram for saddle/source bimodal linear dynamical systems," *Int. J. of Mathematical and Computational Methods* **1**, 345–350.

Ferrer, J., Peña, M. & Susin, A. [2017] "Bifurcation diagram of saddle/spiral bimodal linear systems," *Int. J. Bifurcation and Chaos* **27**, no. 1, 1750005, 13 pp.

Freire, E., Ponce, E., Rodrigo, F. & Torres, F. [1998] "Bifurcation sets of continuous piecewise linear systems with two zones," *Int. J. Bifurcation and Chaos* **8**, 2073–2097.

Freire, E., Pizarro, L. & Rodriguez-Luis, A.J. [2000] "Numerical continuation of homoclinic orbits to nonhyperbolic equilibria in planar systems," *Nonlin. Dyn.* **23**, 353–375.

Llibre, J., Ordonez, M. & Ponce, E. [2013] "On the existence and uniqueness of limit cycles in planar continuous piecewise linear systems without symmetry," *Nonlin. Anal.* **14**, 2002–2012.

Sotomayor, J. & Garcia, R. [2003] "Structural stability of piecewise-linear vector fields," *J. Diff. Eqs.*, **192**, 553–565.

Xu, B., Yang, F., Tang, Y. & Lin, M. [2013] "Homoclinic bifurcations in planar piecewise-linear systems," *Discr. Dyn. Nature and Society*, 732321, 1–9.

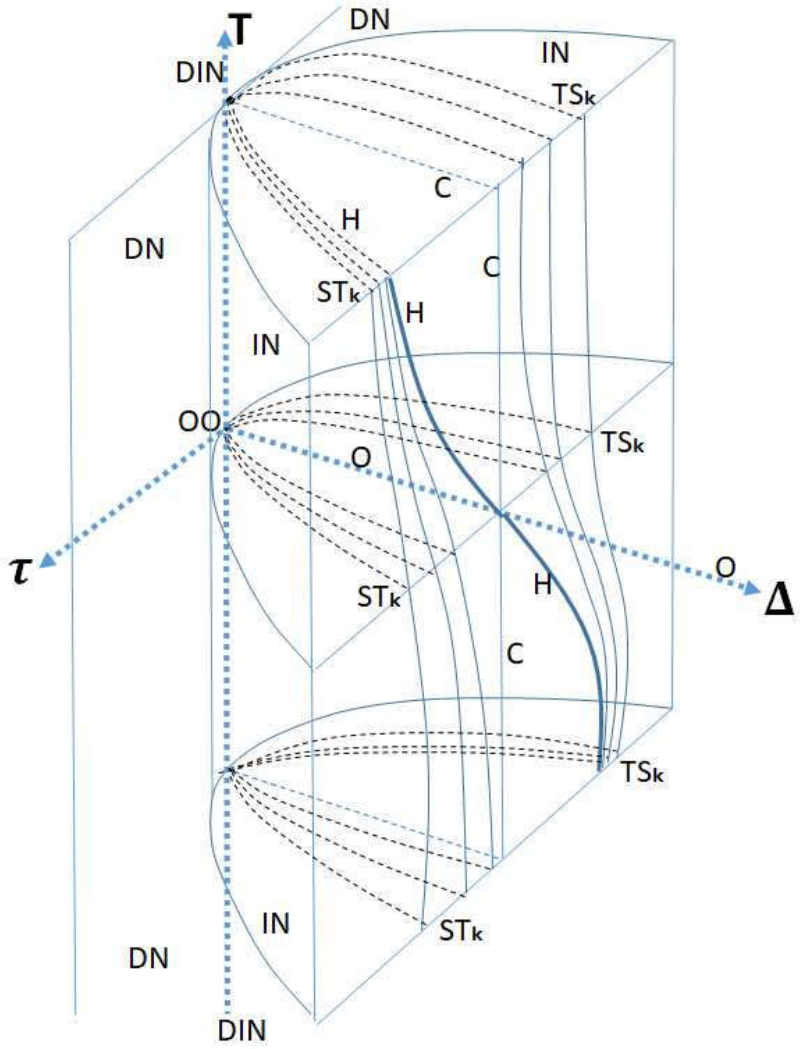

Fig. 11. The 3D bifurcation diagram